ACS APPLIED MATERIALS & INTERFACES

Review

www.acsami.org

High-Resolution Metal Nanopatterning by Means of Switchable Block Copolymer Templates

Nadja C. Bigall,*[,†] Bhanu Nandan,[‡] E. Bhoje Gowd,[§] Andriy Horechyy,[⊥] and Alexander Eychmüller*[,#]

[†]Institute of Physical Chemistry and Electrochemistry, Leibniz Universität Hannover, Callinstraße 3A, D-30167 Hannover, Germany

[‡]Department of Textile Technology, Indian Institute of Technology Delhi, New Delhi 110016, India

[§]Materials Science and Technology Division, CSIR—National Institute for Interdisciplinary Science and Technology, Trivandrum, Kerala, India

[⊥]Leibniz Institute of Polymer Research Dresden, Hohe Straße 6, D-01069 Dresden, Germany

[#]Physical Chemistry, TU Dresden, Bergstraße 66b, D-01062 Dresden, Germany

ABSTRACT: In this review, recent developments in the fabrication of hexagonal and parallel ordered arrays of metallic nanodomains on a substrate are described. We focus on the nanopatterning approach by means of switchable block copolymer thin films. This approach is highly advantageous, because it can lead to extremely regular patterns with metal subunits of only a few nanometers in diameter and center-to-center distances of tens of nanometers. Hence, the resulting 1D or 2D periodic arrays of metal nanodots and nanowires on silicon substrates can be fabricated with extremely high unit densities and on very large areas. The templated deposition of presynthesized metal nanoparticles on functional block copolymers is described in detail. Current challenges are discussed and an outlook for further developments is given.

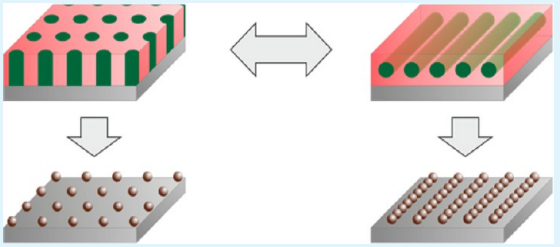

KEYWORDS: *metal nanoparticles, block copolymers, self-assembly, supramolecular assembly, nanopatterning*

INTRODUCTION

Noble metal nanoparticles are in the research focus of many nanomaterial scientists for decades, because they exhibit fascinating, partially size-dependent physical and chemical properties.[1−6] Possible applications of such nanomaterials are, for example, found in catalysis because of their large surface to volume ratio.[7−10] Also, some metal nanoparticles exhibit localized surface plasmon resonances, which result in interesting optical phenomena making such nanoparticles suitable for a broad range of applications in surface-enhanced Raman spectroscopy (SERS), refractive index sensing, and fluorescence enhancement.[11−19] As a result of intense scientific efforts, nowadays various synthetic pathways have been developed to prepare colloidal solutions of noble metal nanoparticles. With one synthetic step, 1×10^{12} or more nanoparticles can be synthesized with similar shapes and sizes, and both size and shape are tunable to a large extent. In many cases, however, these noble metal nanoparticles need to be arranged in a way so that the resulting superstructures still exhibit the advantageous application-oriented physicochemical nanoscopic properties.[20] Desired properties for catalytic applications are good accessibility and highest possible specific surface, leading to mostly voluminous e.g., gel-like non-templated arrangements,[21−26] or to templated nanoparticle arrangements on various kinds of substrates such as fibers for, for example, textile catalysis.[27−29] On the other hand, for sensing applications (such as chemical sensors or SERS-based sensors)[30−32] or the incorporation into high-density data storage devices or small distance conducting paths,[33] the nanoparticles need to be assembled with high precision on flat substrates, and the space between them should be regular and adjustable. For the deposition of particles on substrates the particle-substrate interactions are of high importance and need to be understood in-depth. Recent work focused on the growth kinetics, temperature dependencies, and interactions between metal particles and various substrates such as silicon and silica (amorphous and crystalline), sodium chloride, and various polymers.[34−37] Furthermore, for such highly advanced purposes as the above-mentioned sensing applications, ways need to be explored to tailor and control the periodicity of the nanoparticle assemblies.[38] Conventional particle deposition methods such as spin-coating, spray-coating, or dip-coating will lead to either densely packed nanoparticle arrangements or even nonordered ones. In many cases, so-called self-assembly approaches can be applied leading to either densely packed or voluminous and highly porous architectures, depending on the respective conditions.[39,40] Template-based nanolithography is more suitable when the nanoparticles will be deposited with a certain distance from each other in regular patterns.[41−59] In particular, block copolymer (BCP) template-based nano-

Special Issue: Forum on Polymeric Nanostructures: Recent Advances toward Applications

Received: October 31, 2014
Accepted: January 26, 2015
Published: January 26, 2015

DOI: 10.1021/am507567q
ACS Appl. Mater. Interfaces 2015, 7, 12559−12569

lithography is a powerful tool to achieve control over both the periodicity and the type of arrangement. The latter can be a one-dimensional periodic array (such as fingerprint-like wire-type nanoparticle arrangements) or a two-dimensional (i.e., dotlike) periodic array of the nanoparticles with long-range order. In this technique, the regular periodic structures from self-assembled block copolymers or BCP-based supramolecular complexes are prepared on flat substrates and functionalized with nanoparticles using either in situ or ex situ methods. Depending on the BCP composition, film thickness, treatment conditions, etc., these structures can form ordered lamellae, cylinders, or spheres with periodicities ranging from 5 to 50 nm.[60−64] Alternatively, nanoporous BCP thin films consisting of regular nanometer-sized grooves or pots can be formed by surface reconstruction or, for example, by removal of small molecules.[65−67] The porous BCP templates may also be infiltrated selectively with the colloidal nanoparticles deposited in the grooves or pots because of specific chemical interactions, electrostatic attraction, or capillary forces. Finally, the polymeric template can be removed, e.g., by pyrolysis or plasma treatment, during which small metal nanoparticles fuse or aggregate to larger nanoparticles while still remaining at their deposition sites. The BCP templating method is extremely versatile because, in principle, it is applicable to fabricate a variety of nanostructures via selection of appropriate BCP composition, adjustment of the nanoparticle size and shape and tuning the NP surface chemistry, etc..[41] Additionally, the nanoparticle patterning by means of block copolymer templates with its extremely high resolution is compatible with silicon technology and, therefore, of interest for many industrial applications.[68] In the following, we will discuss recent developments in high-resolution two-dimensional metal nanoparticle patterning by means of block copolymer templates.

RECENT DEVELOPMENTS

a. General Fabrication Procedure. In Figure 1, a schematic illustration of the fabrication procedure is depicted as described in reference 69. The block copolymer thin films are deposited on flat substrates, which is usually achieved by spin- or dip-coating the block copolymer from its solution in a suitable solvent.[70] The formation of self-assembled structures is driven by the immiscibility (microphase separation) of different blocks of BCP competing with the chemical linking between them. Hence, the crucial parameters for the resulting film morphology are the strength of the interaction between the different polymer blocks, their volume fraction, the molecular weight, as well as the film thickness, the substrate surface chemistry, the film preparation, and post-treatment conditions.[71−73] Because as-cast BCP films often display disordered morphologies, thermal or solvent vapor annealing procedures are typically employed to induce the BCP self-assembly and generate ordered structures.[74−77] The ordered patterns can have unit sizes of a few to hundreds of nanometers, whereas the films may be tens to several hundreds of nanometers thick. Subsequently, etching by UV irradiation,[78] removal of low-molecular-weight additives,[79−81] or surface reconstruction steps[66,82,83] have been applied to create the desired pores for subsequent nanoparticle infiltration.

The next step is to place the nanoparticles in these templates so that they exhibit a regular arrangement in 1 or 2 dimensions. For this purpose, in situ or ex situ approaches are optional which will be explained in the following: In situ approaches use the block copolymer thin films as templates for (metal)

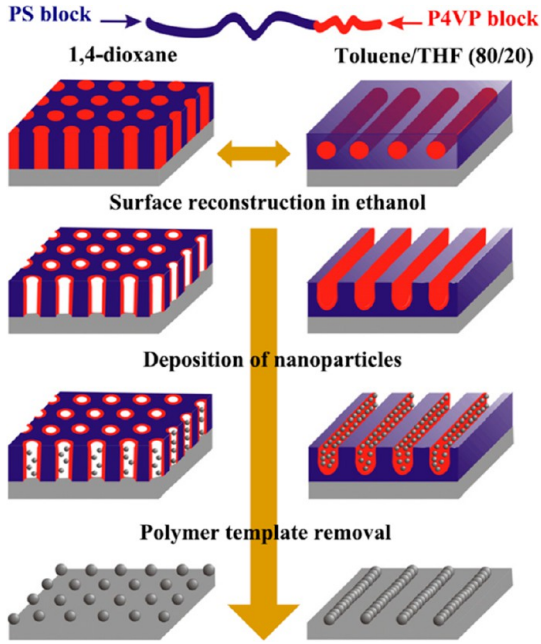

Figure 1. Work steps for the fabrication of 1D or 2D periodic metal nanodot arrays by switchable block copolymer templates. Reprinted (adapted) with permission from ref 69. Copyright 2009 IOP Publishing.

nanopattern formation, which can be achieved by electrodeposition,[66,84,85] atomic layer deposition,[86] infiltration with salts followed by chemical, plasma or light induced reduction,[87−107] chemical vapor deposition and metal deposition from the gas phase.[82,98,108−113] Alternatively, in so-called ex situ approaches, the BCP film templates are directly infiltrated with ready-made nanoparticles from their solutions. Nanoparticle deposition can be realized by many techniques such as, for example, infiltration, the flow stream technique,[114] spray deposition,[115−117] spin-coating, dip-coating, and long-term infiltration, the latter ones being the traditionally and hence still most frequently applied techniques for deposition inside the pores of BCP films. The ex situ approaches have the advantage of being independent from the reaction and diffusion kinetics during the nanocrystal growth, and that they are expandable to many different materials.[118−125] The major advantage and beauty of this powerful technique is that, in principle, the respective nanoparticle building blocks can be controlled in size and shape because of the highly developed colloidal synthesis routes that have been reported over the last 30 years.[3,5,126−132] In the last step, the polymer is removed. This can be achieved by degrading the polymer, with special attention to prevent the nanoparticles from getting removed at the same time or to avoid the nanoparticle agglomeration. We found that removal via pyrolysis in air or by an oxygen plasma had the effect of fusion or aggregation of the metal nanoparticles into larger particles at the sites of the pores.

b. Supramolecular Assembly Approach. The polymers used in our works are the linear diblock copolymers polystyrene-*block*-poly(4-vinylpyridine) (PS-*b*-P4VP) and polystyrene-*block*-poly(2-vinylpyridine) (PS-*b*-P2VP) of varied molecular weight and block ratios. For instance, asymmetric BCPs, which form cylindrical microdomains, allow us to fabricate nanostructured thin films with their microdomain orientation being switchable between perpendicular and parallel to the substrate. Starting from the substrate perpendicular

DOI: 10.1021/am507567q
ACS Appl. Mater. Interfaces 2015, 7, 12559−12569

cylindrical morphology, we were able to generate highly ordered metal nanodot arrays with a periodicity on the nanometer scale.[80] The switchability of the thin films from 1D periodic to 2D periodic and back by means of simple solvent vapor annealing (see Figure 2) has the advantage that

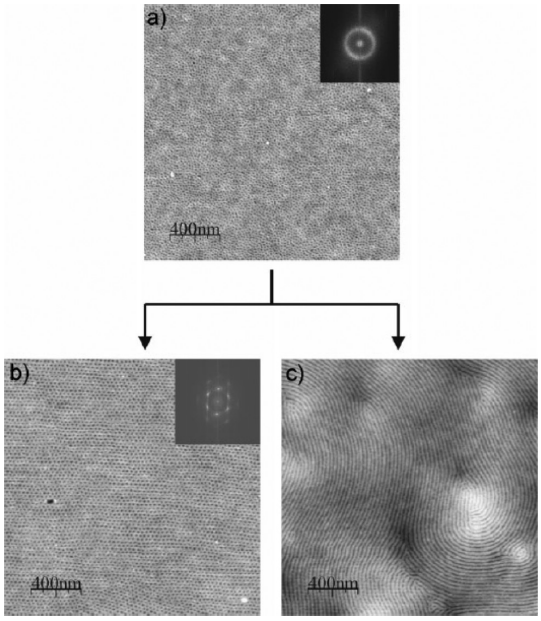

Figure 2. Morphologies (measured by atomic force microscopy) of the supramolecular assemblies from PS-*b*-P4VP(HABA) thin films after 2-(4′-hydroxybenzeneazo) benzoic acid (HABA) removal. (a) Dip-coated films from 1,4-dioxane solution, and after annealing in (b) 1,4-dioxane and (c) chloroform vapors. Reprinted with permission from ref 80. Copyright 2009 Wiley−VCH.

two different nanoparticle assemblies can be achieved using the same technique. In this case, a supramolecular complex of PS-*b*-P4VP and low molecular weight additive, 2-(4′-hydroxybenzeneazo) benzoic acid (HABA) were assembled onto silicon wafers. The pores were created by removal of HABA after rinsing with methanol. In the case of perpendicularly oriented microdomains, after solvent vapor annealing and HABA removal, a quasi-perfect hexagonal pore pattern with an area of several square microns can be obtained with the areal pore density of approximately 1665 μm^{-2} (Figure 2b). Oppositely, in the case of substrate-parallel-oriented microdomains, a homogeneous pattern of parallel grooves with certain curvatures appeared after solvent vapor annealing and HABA removal, leading to a fingerprint-type pattern. Determined by AFM, the center-to-center distance of the pores as was as small 24.5 nm ± 1.5 nm and 30 nm ± 1.5 nm for perpendicular and parallel aligned pores and grooves, respectively.

Subsequent infiltration of the pattern with palladium nanoparticles for 1 day followed by rinsing with water led to the accumulation of several palladium nanoparticles per pore, having the walls covered with the poly(4-vinylpyridine) block capable to coordinate the palladium nanoparticles. In this work, the palladium NPs of 2 nm in diameter were synthesized by citrate and sodium borohydride reduction of hexachloropalladate in aqueous solution according to previously reported procedures.[132−134] By atomic force microscopy, almost no palladium nanoparticles were found on the surface of the BCP films after rinsing with water. Instead, the presence of the palladium located inside the pores was proven by X-ray photoelectron spectroscopy. The reason for this observation is that the palladium nanoparticles were able to enter the hydrophilic P4VP grafted pores due to their good wetting properties, and that the P4VP chains coordinate the palladium nanoparticles, while the matrix-forming PS block does not exhibit such affinity toward Pd NPs, so that residual unbound palladium nanoparticles could be removed from the surface of the film easily by washing with water.

To remove the polymer templates remaining, we conducted pyrolysis of the samples at 450 °C in air or treated the samples with oxygen plasma maintaining the location of the deposited palladium particles on the substrates. We found that UV-cross-linking of the polymer films prior to template removal was crucial to keep the palladium nanoparticles localized at their respective pore sites. The center-to-center distances of the periodic arrays determined from the analysis of SEM images were 27.5 nm ± 1.5 nm similar to that of the polymer template system. At elevated temperatures, the palladium nanoparticles had fused or aggregated at the pore sites during template removal. Thus, the residual 2D periodic array of palladium on the silicon wafer exhibited a pattern of metallic nanodots of 7 nm ± 2 nm in diameter (from high-resolution SEM, see also Figure 3a) and at least 2 nm in height (measured by AFM).

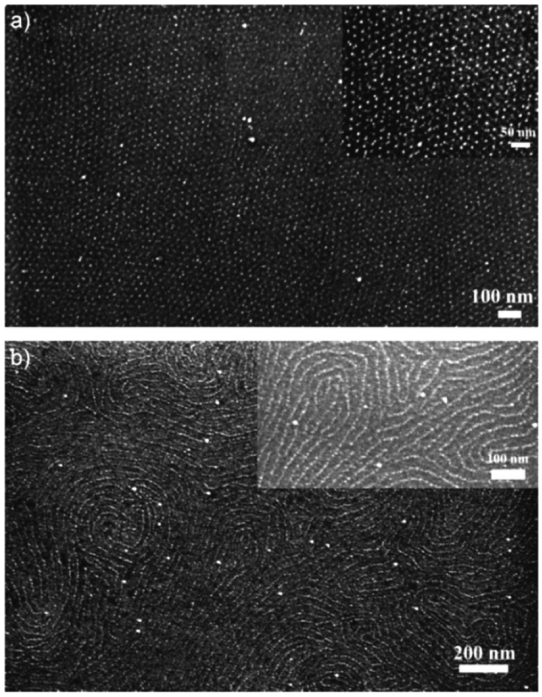

Figure 3. SEM images of (a) 2D periodic arrays and (b) 1D periodic "fingerprint-type" parallel patterns of metallic nanodomains on a silicon wafer. Reprinted with permission from ref 80. Copyright 2009 Wiley−VCH.

Also in the case of substrate parallel domain orientation the pattern of the residual palladium after polymer removal followed the original groove pattern with palladium nanoparticles fusing to a fingerprint-type wirelike arrangement of 8 nm ± 1.5 nm in thickness (SEM) and at least 3 nm in height (AFM) (see Figure 3b). Hence, in this work we had shown that by switchable-polymer templating we were able to position palladium particles with nanometer precision in one- and two-dimensional periodic arrays onto silicon wafers with lateral

DOI: 10.1021/am507567q
ACS Appl. Mater. Interfaces 2015, 7, 12559−12569

periodicity below 30 nm being one of the smallest periodicities at that time.

c. Surface Reconstruction Approach. In a subsequent set of experiments,[69] the fabrication of metallic nanostructures via the block copolymer template approach was modified by using the PS-*b*-P4VP BCP with shorter PS and longer P4VP blocks, respectively, but this time without the addition of the low molecular weight HABA molecule. In this case, 1,4-dioxane and a toluene/tetrahydrofuran(THF) mixture (80:20) were employed for solvent vapor annealing in order to yield highly ordered BCP microdomains being perpendicular and parallel oriented to the substrate (Figure 1). Upon dipping these thin films into ethanol, cylindrical pores or parallel aligned grooves appeared, respectively. Infiltration with nanoparticles for 1 h only was necessary to achieve dense nanoparticle loading. In this case, the density of P4VP chains on the pore walls was higher than that of the BCP templates obtained by HABA removal. Hence, more palladium nanoparticles are coordinated with the longer P4VP chains, which resulted in more dense nanostructures compared to the procedure discussed in the preceding section. The final palladium nanodots and nanowires had a similar regularity and comparably small lateral distances (26 nm ± 2 and 30 nm ± 2 nm for nanodots and nanowires, respectively), exactly matching the respective polymer template pattern. The nanodots and nanowires had diameters (widths) of 12 nm ± 1 nm, again being the result of site localization of the nanoparticles during the pyrolysis step in combination with fusion of several palladium nanoparticles located at each pore at elevated temperatures.

As further proof of the principle, BCP template-assisted deposition of nanoparticles was further extended by employing a PS-*b*-P4VP with different block ratios: whereas the overall molar mass of the BCP was kept almost unaltered, the volume fraction of the P4VP block was changed (increased/decreased) as compared to the previously used BCPs. When dissolved in a toluene/THF mixture, the BCP formed micelles having a core composed of collapsed P4VP chains with a corona formed by the swollen PS block. These micelles could be transferred onto the silicon substrate by dip-coating. Surface reconstruction in ethanol vapor led to the formation of a dimple-type inverted micelle pattern. This type of thin film, again, represented an array of nanoscaled regular holes with the same periodicity of 40 nm ± 2 nm as the micellar film acting as a template for the infiltration of palladium nanoparticles (Figure 4). After annealing the pristine polymer micellar film in 1,4-dioxane, a perpendicular aligned structure from lamellae was observed, which again could successfully be applied as a template for deposition of palladium nanoparticles. Even though the order of both the surface reconstructed system and of the resulting palladium dot array after polymer removal was not as high as that received with the previously applied block copolymers, it is noted that also here the palladium deposition had exactly reproduced the polymer template pattern, as was confirmed from the power spectral density (PSD) analysis of AFM images (not shown). This experiment indicated that direct templating (i.e., without an application of low molecular weight additives such as HABA) by simply self-assembling and surface reconstructing PS-*b*-P4VP polymers is advantageous in comparison to using templates created by removing a small molecule. This is because the technique can be expanded to a large variety of different PS-*b*-P4VP polymers varying in molecular weight and in the volume fractions of the two polymer blocks. We have proven this further by employing PS-*b*-P4VP BCP with a total molecular weight being approximately 1.5 times higher than in the previous cases.[135] By employing this block copolymer composed of the same building blocks, again arrays of highly regular hexagonally closed packed cylinders were fabricated with a comparatively higher center-to-center spacing of 56 nm ± 2 nm and an average diameter of the P4VP cylinders of 26 nm ± 2 nm. Since, also in this case, we were able to employ these regular films as templates for noble metal nanoparticles, this indicates that by changing the volume fraction or chain length of the P4VP, the final size of the nanodots after polymer removal can be adjusted, so that high density arrays of noble metal nanodots with feature sizes up to 10 nm can be easily reached by an appropriate choice of the starting polymer.

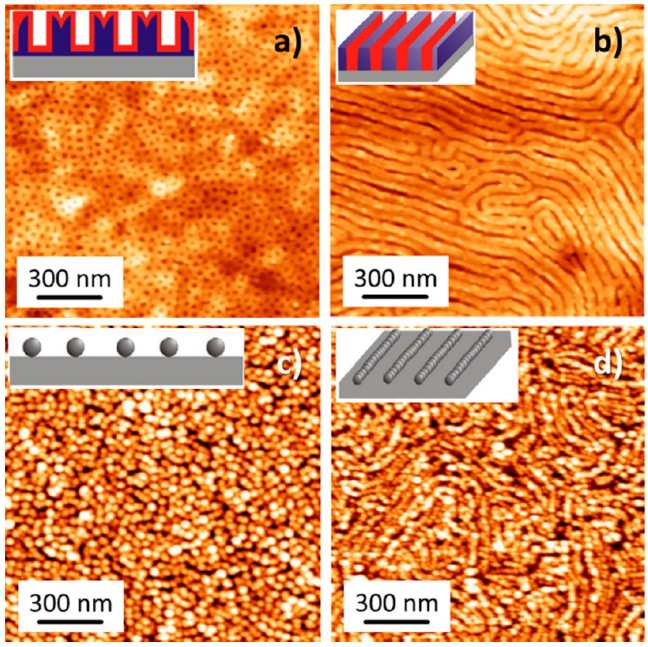

Figure 4. Schematic diagrams (insets) and AFM height images of surface-reconstructed (a) micelles and (b) lamellae before the deposition of nanoparticles, and of palladium nanodots after the (c) micellar and (d) lamellar polymer template removal. Adapted with permission from ref 69. Copyright 2009 IOP Publishing.

Using the same BCP thin films, we also reported on the extension of the method to gold and platinum nanoparticles.[135] However, in this study, the BCP thin films were directly dipped into the nanoparticle dispersion before creating the nanopores or grooves. This study showed that the strength of the coordination of the P4VP to the metal nanoparticles is crucial for the extent of the nanoparticle loading in the P4VP domains during the nanoparticle infiltration as well as on their stability upon post-treatment. For instance, in the case of palladium NPs, their interaction with P4VP was not strong enough to keep the palladium nanoparticles on the surface of the P4VP domains, when PdNP/PS-*b*-P4VP composite films were etched from the silicon substrates using an aqueous solution of sodium hydroxide (see Figure 5), so that by TEM it was not possible to clearly identify the presence of the palladium nanoparticles at the P4VP domain sites (see Figure 5c). However, we have shown by SEM that palladium infiltration takes place and also the highly ordered palladium nanodot array remains on the substrate after polymer template removal (see Figure 5f along with the observations discussed above). In contrast, gold and platinum nanoparticles could be identified in TEM images

DOI: 10.1021/am507567q
ACS Appl. Mater. Interfaces 2015, 7, 12559−12569

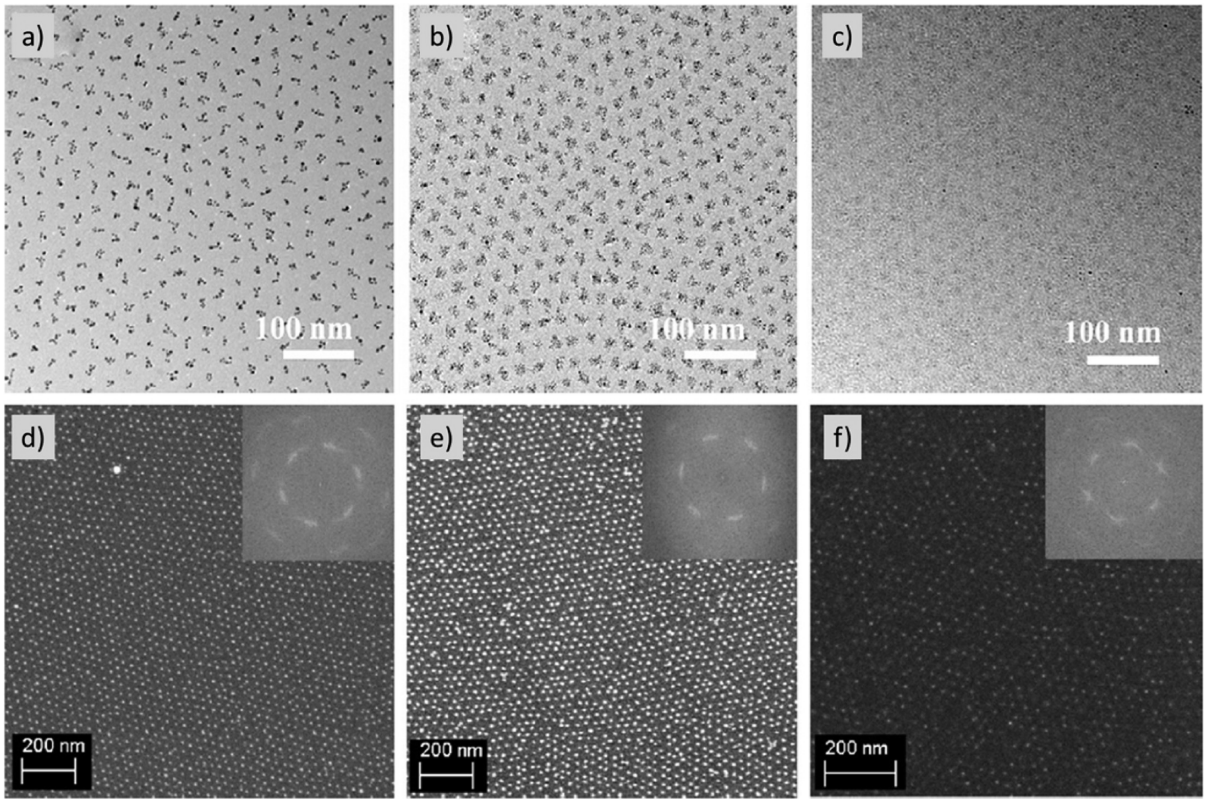

Figure 5. Transmission electron micrographs after floating the (a) gold, (b) platinum, and (c) palladium infiltrated polymer films by means of sodium hydroxide, and SEM images of the resulting highly ordered nanodot arrays of (d) gold, (e) platinum, and (f) palladium. Reprinted (adapted) with permission from ref 135. Copyright 2010 Elsevier.

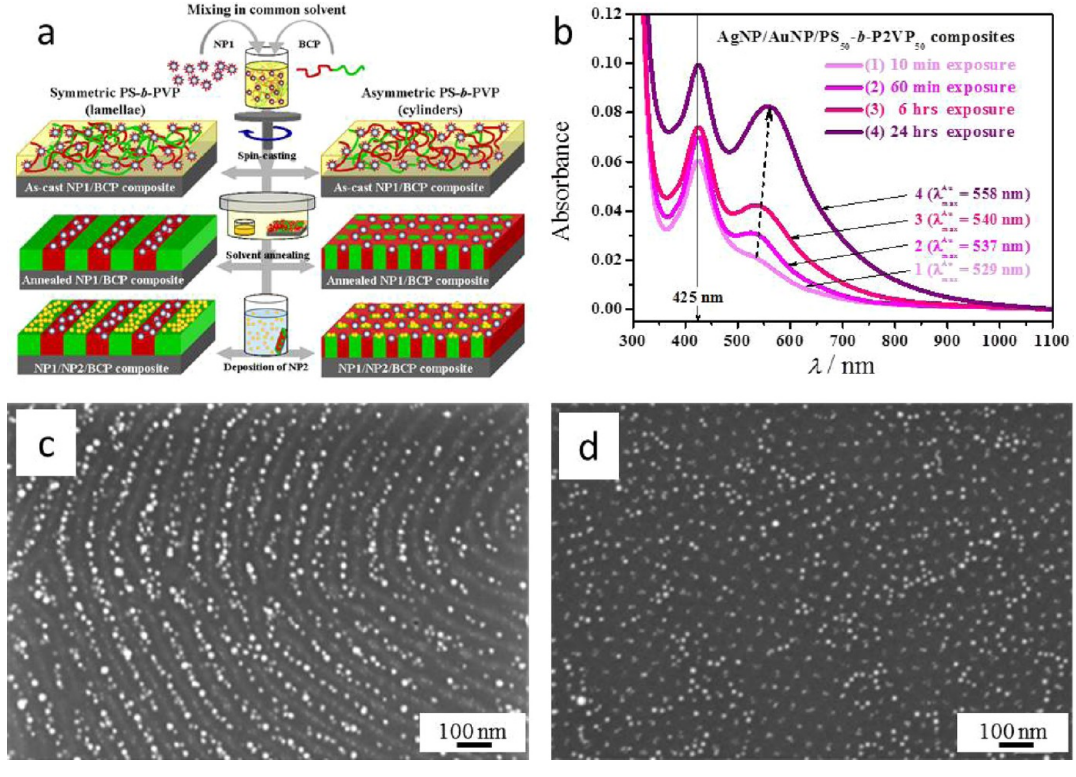

Figure 6. (a) Schematic illustration of the stepwise approach used for patterning of two types of presynthesized nanoparticles exploiting block copolymer self-assembly. (b) UV−vis spectra of ternary AgNP/AuNP/PS_{50}-*b*-$P2VP_{50}$ composites measured after different times of AuNP deposition. (c, d) SEM images of (c) lamellar AgNP/AuNP/PS_{50}-*b*-$P2VP_{50}$ and (d) cylindrical AgNP/AuNP/PS_{57}-*b*-$P4VP_{18}$ composites). Reprinted (adapted) with permission from ref 150. Copyright 2013 Wiley−VCH.

DOI: 10.1021/am507567q
ACS Appl. Mater. Interfaces 2015, 7, 12559−12569

easily (Figure 5a, b). The number of nanoparticles placed on each domain could be counted by analyzing TEM images (Figure 5a, b). For example, in the case of gold nanoparticles, the average number of nanoparticles found on each domain is 4−5 (Figure 5a). By pyrolysis or plasma treatment, these nanoparticles fused to larger nanoparticles by retaining the deposition site. The loading of the nanoparticles was different for all these three noble metal nanoparticle materials resulting in differently sized final gold, platinum, and palladium nanodots (6, 6, and 4 nm in height and 15, 16, and 4 nm in width, respectively), maintaining at the same time equal center-to-center interdot distances. This was attributed both to the variations in the coordination affinity of P4VP to the different noble metals investigated and to variations in the nanoparticle sizes (ranging from 2.5 to 3.8 nm in diameter), leading to different loadings on the surface of the P4VP domains.

We can, hence, conclude that the affinity of the P4VP block toward the noble metal is crucial. Moreover, the affinity is much higher to gold and platinum than to palladium. These observations were further confirmed by infiltrating, as described above, PS-*b*-P4VP micellar films with all three different types of nanoparticles. Here, the micellar film was used without any surface reconstruction. For this kind of polymer templates, for which the nanoparticles are expected to assemble on the top of each micelle, nearly no palladium nanoparticles were found in SEM investigations, whereas for gold and for platinum nanoparticles, regular patterns of the nanoparticles located at the site of each micelle were observed.

d. Dual Nanoparticle Patterning. By altering the interactions between the nanoparticles and the polymer chains which crucially influence the site of the nanoparticle assembly,[42,136−146] it was also possible to incorporate at the same time two different kinds of nanoparticles and, hence, create a ternary nanocomposite structure by controlling the nanoparticle surface chemistry.[147−154] It is thereby favorable to assemble the different types of nanoparticles within the two different domains of the block copolymer template. In our approach[150] we have used two types of nanoparticles having affinity toward different blocks of PS-*b*-P4VP (PS-*b*-P2VP). Schematically, the whole strategy is shown in Figure 6a. As a first type of nanoparticles, we synthesized oleylamine-stabilized Ag NPs and then conducted a ligand exchange step so that finally they were covered with polystyrene ligands.[155] Thus, when mixing these PS-coated nanoparticles with PS-*b*-P4VP or PS-*b*-P2VP BCPs of different chain lengths and architectures the silver nanoparticles were expected to be localized in the polystyrene domains during the formation of self-assembled polymer structures. A similar strategy has been applied previously by other groups in order to incorporate various types of nanoparticles into block copolymer films as well as in bulk.[123,124,156−158] Thus, Ag NP/BCP nanocomposite thin films could be annealed in 1,4-dioxane vapor so that regular composite structures are formed with the silver nanoparticles being located in the polystyrene domains. Hence, in the next step the AgNP/PS-*b*-P4(2)VP composite thin films could be used as templates for depositing citrate stabilized Au, Pt and Pd nanoparticles which, like in all aforementioned cases, assembled at the PVP sites (see Figure 6c for parallel and Figure 6d for 2 D aligned arrays). With this technique, a lateral separation of the silver nanoparticles from the gold, platinum or palladium nanoparticles could be achieved. Because of the remarkable difference in size, the presence and lateral position of each kind of nanoparticles could be identified very easily, e.g., using conventional SEM or TEM. These resulting ternary composite thin films from two different nanoparticle species and a block copolymer (NP1/NP2/BCP) exhibited optical properties similar to those of their nanoparticle building blocks with only a slight shift of the localized surface plasmon resonance maxima of the gold NPs toward longer wavelengths, which was expected due to particle−particle interactions (see Figure 6b).[159] It is noted that we observed some distortions of the hexagonal order of the P4VP cylinders after loading of the polymer with silver nanoparticles.[150] Such distortions of microdomain order are attributed to the relatively large size of the silver nanoparticles and have also been previously reported for other nanoparticle-filled systems.[160,161] Thus, by this approach we succeeded in incorporating two different types of metal nanoparticles by employing a two-step deposition process in combination with the control over the nanoparticle surface chemistry, which is of utmost importance for applications in which two differing nanoparticle properties are needed in close but separated and densely packed proximity.

CONCLUSION AND OUTLOOK

We have shown a variety of recent experimental approaches toward achieving a precise control over the spatial organization of metal nanodomains by means of switchable block copolymer thin film templating of presynthesized metal nanoparticles. We consider this process being a possible route to develop device components in the future. With the techniques described, it is possible to tune the lateral distance and type of arrangement through the adequate choice of polymer, polymer block ratios and solvent treatments. Furthermore, by exploiting the surface chemistry of the metal nanoparticles, we have gained control over the attractive and repulsive interactions of the nanoparticles with the respective building blocks which leads to a control over the site of nanoparticle deposition within the polymer thin film. After polymer removal, regular arrays of nanowires or hexagonally ordered nanodots with controlled lateral spacing and tunable center-to-center distance, in some cases below 30 nm, can be achieved. The noble metal materials employed ranged from palladium to gold and platinum for preferential depositions at the PVP site and to silver for deposition in the PS domains.

However, certainly there are still a variety of tasks to be tackled. The next objectives will be to further reduce the periodicities to even smaller values and to achieve even larger regular areas with defect densities as low as possible. Further improvement of the control over the preferential attraction and repulsion of the nanoparticles to the respective polymer block will lead to a facile expansion to other nanomaterial depositions. A still remaining task is to develop further polymer removal methods after nanoparticle infiltration. So far, in our method, the polymer is mostly removed at elevated temperatures, leading to melting and fusion of the nanoparticles. If we want to profit from the large spectrum of different nanomaterials with different shapes coming from advanced colloidal nanoparticle synthesis routes, a polymer removal method without altering the nanoparticle shape and physical properties is desirable. Therefore, further research is needed to develop polymers that can be easily removed by chemical degradation and at the same time leave the nanoparticles unaltered.

AUTHOR INFORMATION

Corresponding Authors

*E-mail: nadja.bigall@pci.uni-hannover.de.

DOI: 10.1021/am507567q
ACS Appl. Mater. Interfaces 2015, 7, 12559−12569

*E-mail: alexander.eychmueller@chemie.tu-dresden.de.

Author Contributions

The manuscript was written through contributions of all authors. All authors have given approval to the final version of the manuscript.

Funding

German Federal Ministry of Education and Research (BMBF) support code 03X5525.

Notes

The authors declare no competing financial interest.

■ ACKNOWLEDGMENTS

This work is dedicated to Professor Manfred Stamm on the occasion of his 65th birthday. The authors are grateful to all who contributed to the original papers, which constitute the basis of the present review. N.C.B. is grateful for financial support from the German Federal Ministry of Education and Research (BMBF) within the framework of the program NanoMatFutur (support code 03X5525). E.B.G thanks the Department of Science and Technology (Government of India) for the award of Ramanujan fellowship.

■ ABBREVIATIONS

BCP, block copolymer; NPs, nanoparticles; 1D, one-dimensional; 2D, two-dimensional; PS, polystyrene; P4VP, poly(4-vinylpyridine); P2VP, poly(2-vinylpyridine); PS-*b*-P4VP, polystyrene-*block*-poly(4-vinylpyridine); HABA, 2-(4′-hydroxybenzeneazo) benzoic acid; THF, tetrahydrofuran; AFM, atomic force microscopy; TEM, transmission electron microscopy; SEM, scanning electron microscopy; PS-*b*-P2VP, PS-*block*-poly(2-vinylpyridine); kDa, kilo Dalton

■ REFERENCES

(1) El-Sayed, M. A. Small Is Different: Shape-, Size-, and Composition-Dependent Properties of Some Colloidal Semiconductor Nanocrystals. *Acc. Chem. Res.* **2004**, *37*, 326−333.
(2) Link, S.; El-Sayed, M. A. Spectral Properties and Relaxation Dynamics of Surface Plasmon Electronic Oscillations in Gold and Silver Nanodots and Nanorods. *J. Phys. Chem. B* **1999**, *103*, 8410−8426.
(3) Tao, A. R.; Habas, S.; Yang, P. Shape Control of Colloidal Metal Nanocrystals. *Small* **2008**, *4*, 310−325.
(4) Bigall, N. C.; Härtling, T.; Klose, M.; Simon, P.; Eng, L. M.; Eychmüller, A. Monodisperse Platinum Nanospheres with Adjustable Diameters from 10 to 100 nm: Synthesis and Distinct Optical Properties. *Nano Lett.* **2008**, *8*, 4588−4592.
(5) Bigall, N. C.; Parak, W. J.; Dorfs, D. Fluorescent, Magnetic and Plasmonic−Hybrid Multifunctional Colloidal Nano Objects. *Nano Today* **2012**, *7*, 282−296.
(6) Ziegler, C.; Eychmüller, A. Seeded Growth Synthesis of Uniform Gold Nanoparticles with Diameters of 15−300 nm. *J. Phys. Chem. C* **2011**, *115*, 4502−4506.
(7) Li, Y.; El-Sayed, M. A. The Effect of Stabilizers on the Catalytic Activity and Stability of Pd Colloidal Nanoparticles in the Suzuki Reactions in Aqueous Solution. *J. Phys. Chem. B* **2001**, *105*, 8938−8943.
(8) Narayanan, R.; El-Sayed, M. A. Shape-Dependent Catalytic Activity of Platinum Nanoparticles in Colloidal Solution. *Nano Lett.* **2004**, *4*, 1343−1348.
(9) Balanta, A.; Godard, C.; Claver, C. Pd Nanoparticles for C-C Coupling Reactions. *Chem. Soc. Rev.* **2011**, *40*, 4973−4985.
(10) Campelo, J. M.; Luna, D.; Luque, R.; Marinas, J. M.; Romero, A. A. Sustainable Preparation of Supported Metal Nanoparticles and Their Applications in Catalysis. *ChemSusChem* **2009**, *2*, 18−45.
(11) Anger, P.; Bharadwaj, P.; Novotny, L. Enhancement and Quenching of Single-Molecule Fluorescence. *Phys. Rev. Lett.* **2006**, *96*, 113002.
(12) Kuehn, S.; Hakanson, U.; Rogobete, L.; Sandoghdar, V., Enhancement of Single-Molecule Fluorescence Using a Gold Nanoparticle as an Optical Nanoantenna. *Phys. Rev. Lett.* **2006**, *97*.
(13) Nie, S. M.; Emery, S. R. Probing Single Molecules and Single Nanoparticles by Surface-Enhanced Raman Scattering. *Science* **1997**, *275*, 1102−1106.
(14) Campion, A.; Kambhampati, P. Surface-Enhanced Raman Scattering. *Chem. Soc. Rev.* **1998**, *27*, 241−250.
(15) Lal, S.; Link, S.; Halas, N. J. Nano-Optics from Sensing to Waveguiding. *Nat. Photonics* **2007**, *1*, 641−648.
(16) Mulvaney, P. Surface Plasmon Spectroscopy of Nanosized Metal Particles. *Langmuir* **1996**, *12*, 788−800.
(17) Huang, X.; Jain, P. K.; El-Sayed, I. H.; El-Sayed, M. A. Plasmonic Photothermal Therapy (Pptt) Using Gold Nanoparticles. *Lasers Med. Sci.* **2008**, *23*, 217−228.
(18) Jain, P. K.; Huang, X.; El-Sayed, I. H.; El-Sayed, M. A. Noble Metals on the Nanoscale: Optical and Photothermal Properties and Some Applications in Imaging, Sensing, Biology, and Medicine. *Acc. Chem. Res.* **2008**, *41*, 1578−1586.
(19) Willets, K. A.; Van Duyne, R. P. Localized Surface Plasmon Resonance Spectroscopy and Sensing. *Annu. Rev. Phys. Chem.* **2007**, *58*, 267−297.
(20) Bigall, N. C.; Eychmüller, A. Synthesis of Noble Metal Nanoparticles and Their Non-Ordered Superstructures. *Philos. Trans. R. Soc. London, Ser. A* **2010**, *368*, 1385−1404.
(21) Liu, W.; Herrmann, A.-K.; Bigall, N. C.; Rodriguez, P.; Wen, D.; Oezaslan, M.; Schmidt, T.; Gaponik, N.; Eychmüller, A. Noble Metal Aerogels — Synthesis, Characterization, and Application as Electrocatalysts. *Acc. Chem. Res.* **2015**, DOI: 10.1021/ar500237c.
(22) Herrmann, A.-K.; Formanek, P.; Borchardt, L.; Klose, M.; Giebeler, L.; Eckert, J.; Kaskel, S.; Gaponik, N.; Eychmüller, A. Multimetallic Aerogels by Template-Free Self-Assembly of Au, Ag, Pt, and Pd Nanoparticles. *Chem. Mater.* **2014**, *26*, 1074−1083.
(23) Bigall, N. C.; Herrmann, A. K.; Vogel, M.; Rose, M.; Simon, P.; Carrillo-Cabrera, W.; Dorfs, D.; Kaskel, S.; Gaponik, N.; Eychmüller, A. Hydrogels and Aerogels from Noble Metal Nanoparticles. *Angew. Chem., Int. Ed.* **2009**, *48*, 9731−9734.
(24) Hendel, T.; Lesnyak, V.; Kuhn, L.; Herrmann, A. K.; Bigall, N. C.; Borchardt, L.; Kaskel, S.; Gaponik, N.; Eychmüller, A. Mixed Aerogels from Au and CdTe Nanoparticles. *Adv. Funct. Mater.* **2013**, *23*, 1903−1911.
(25) Liu, W.; Herrmann, A. K.; Geiger, D.; Borchardt, L.; Simon, F.; Kaskel, S.; Gaponik, N.; Eychmüller, A. High-Performance Electrocatalysis on Palladium Aerogels. *Angew. Chem., Int. Ed.* **2012**, *51*, 5743−5747.
(26) Liu, W.; Rodriguez, P.; Borchardt, L.; Foelske, A.; Yuan, J. P.; Herrmann, A. K.; Geiger, D.; Zheng, Z. K.; Kaskel, S.; Gaponik, N.; Kotz, R.; Schmidt, T. J.; Eychmüller, A. Bimetallic Aerogels: High-Performance Electrocatalysts for the Oxygen Reduction Reaction. *Angew. Chem., Int. Ed.* **2013**, *52*, 9849−9852.
(27) Zhao, Y.; Sugunan, A.; Rihtnesberg, D. B.; Wang, Q.; Toprak, M. S.; Muhammed, M. Size-Tuneable Synthesis of Photoconducting Poly-(3-Hexylthiophene) Nanofibres and Nanocomposites. *Phys. Status Solidi C* **2012**, *9*, 1546−1550.
(28) Sugunan, A.; Guduru, V. K.; Uheida, A.; Toprak, M. S.; Muhammed, M. Radially Oriented Zno Nanowires on Flexible Poly-L-Lactide Nanofibers for Continuous-Flow Photocatalytic Water Purification. *J. Am. Ceram. Soc.* **2010**, *93*, 3740−3744.
(29) Lee, J.-W.; Mayer-Gall, T.; Opwis, K.; Song, C. E.; Gutmann, J. S.; List, B. Organotextile Catalysis. *Science* **2013**, *341*, 1225−1229.
(30) Wolkenhauer, M.; Bumbu, G.-G.; Cheng, Y.; Roth, S. V.; Gutmann, J. S. Investigation of Micromechanical Cantilever Sensors with Microfocus Grazing Incidence Small-Angle X-Ray Scattering. *Appl. Phys. Lett.* **2006**, *89*, 054101 (054103 pp)..

DOI: 10.1021/am507567q
ACS Appl. Mater. Interfaces 2015, 7, 12559−12569

(31) Amarandei, G.; O'Dwyer, C.; Arshak, A.; Corcoran, D. Fractal Patterning of Nanoparticles on Polymer Films and Their Sers Capabilities. *ACS Appl. Mater. Interfaces* **2013**, *5*, 8655−8662.
(32) Santoro, G.; Yu, S.; Schwartzkopf, M.; Zhang, P.; Koyiloth Vayalil, S.; Risch, J. F. H.; Rübhausen, M. A.; Hernández, M.; Domingo, C.; Roth, S. V. Silver Substrates for Surface Enhanced Raman Scattering: Correlation between Nanostructure and Raman Scattering Enhancement. *Appl. Phys. Lett.* **2014**, *104*, 243107 (243105 pp)..
(33) Martin, N.; Bigall, N. C.; Monch, I.; Gemming, T.; Eychmüller, A.; Mattheis, R.; Schafer, R.; Schultz, L.; McCord, J. Enhanced Nucleation of Vortices in Soft Magnetic Materials Prepared by Silica Nanosphere Lithography. *Adv. Funct. Mater.* **2011**, *21*, 891−896.
(34) Ruffino, F.; Torrisi, V.; Marletta, G.; Grimaldi, M. G. Growth Morphology of Nanoscale Sputter-Deposited Au Films on Amorphous Soft Polymeric Substrates. *Appl. Phys. A: Mater. Sci. Process.* **2011**, *103*, 939−949.
(35) Maret, M.; Liscio, F.; Makarov, D.; Doisneau-Cottignies, B.; Ganss, F.; Missiaen, J.-M.; Albrecht, M. Growth Temperature Effect on the Structure of Copt Islands on Nacl(001) Studied by Grazing-Incidence Small-Angle X-Ray Scattering. *J. Appl. Crystallogr.* **2014**, *47*, 102−109.
(36) Schwartzkopf, M.; Buffet, A.; Korstgens, V.; Metwalli, E.; Schlage, K.; Benecke, G.; Perlich, J.; Rawolle, M.; Rothkirch, A.; Heidmann, B.; Herzog, G.; Muller-Buschbaum, P.; Rohlsberger, R.; Gehrke, R.; Stribeck, N.; Roth, S. V. From Atoms to Layers: In Situ Gold Cluster Growth Kinetics During Sputter Deposition. *Nanoscale* **2013**, *5*, 5053−5062.
(37) Portale, G.; Sciortino, L.; Albonetti, C.; Giannici, F.; Martorana, A.; Bras, W.; Biscarini, F.; Longo, A. Influence of Metal-Support Interaction on the Surface Structure of Gold Nanoclusters Deposited on Native Siox/Si Substrates. *Phys. Chem. Chem. Phys.* **2014**, *16*, 6649−6656.
(38) Grzelczak, M.; Vermant, J.; Furst, E. M.; Liz-Marzan, L. M. Directed Self-Assembly of Nanoparticles. *ACS Nano* **2010**, *4*, 3591−3605.
(39) Liang, H.-W.; Liu, J.-W.; Qian, H.-S.; Yu, S.-H. Multiplex Templating Process in One-Dimensional Nanoscale: Controllable Synthesis, Macroscopic Assemblies, and Applications. *Acc. Chem. Res.* **2013**, *46*, 1450−1461.
(40) Liu, J.-W.; Liang, H.-W.; Yu, S.-H. Macroscopic-Scale Assembled Nanowire Thin Films and Their Functionalities. *Chem. Rev.* **2012**, *112*, 4770−4799.
(41) Segalman, R. A. Patterning with Block Copolymer Thin Films. *Mater. Sci. Eng. R* **2005**, *48*, 191−226.
(42) Haryono, A.; Binder, W. H. Controlled Arrangement of Nanoparticle Arrays in Block-Copolymer Domains. *Small* **2006**, *2*, 600−611.
(43) Melosh, N. A.; Davidson, P.; Chmelka, B. F. Monolithic Mesophase Silica with Large Ordering Domains. *J. Am. Chem. Soc.* **2000**, *122*, 823−829.
(44) Mansky, P.; Harrison, C. K.; Chaikin, P. M.; Register, R. A.; Yao, N. Nanolithographic Templates from Diblock Copolymer Thin Films. *Appl. Phys. Lett.* **1996**, *68*, 2586−2588.
(45) Zschech, D.; Milenin, A. P.; Scholz, R.; Hillebrand, R.; Sun, Y.; Uhlmann, P.; Stamm, M.; Steinhart, M.; Goesele, U. Transfer of Sub-30-Nm Patterns from Templates Based on Supramolecular Assemblies. *Macromolecules* **2007**, *40*, 7752−7754.
(46) Whitesides, G. M.; Mathias, J. P.; Seto, C. T. Molecular Self-Assembly and Nanochemistry - a Chemical Strategy for the Synthesis of Nanostructures. *Science* **1991**, *254*, 1312−1319.
(47) Hamley, I. W. Nanotechnology with Soft Materials. *Angew. Chem., Int. Ed.* **2003**, *42*, 1692−1712.
(48) Harrison, C.; Park, M.; Chaikin, P. M.; Register, R. A.; Adamson, D. H. Lithography with a Mask of Block Copolymer Microstructures. *J. Vac. Technol. B* **1998**, *16*, 544−552.
(49) Li, R. R.; Dapkus, P. D.; Thompson, M. E.; Jeong, W. G.; Harrison, C.; Chaikin, P. M.; Register, R. A.; Adamson, D. H. Dense Arrays of Ordered Gaas Nanostructures by Selective Area Growth on Substrates Patterned by Block Copolymer Lithography. *Appl. Phys. Lett.* **2000**, *76*, 1689−1691.
(50) Krishnamoorthy, S.; Hinderling, C.; Heinzelmann, H. Nanoscale Patterning with Block Copolymers. *Mater. Today* **2006**, *9*, 40−47.
(51) Krishnamoorthy, S.; Pugin, R.; Brugger, J.; Heinzelmann, H.; Hoogerwerf, A. C.; Hinderling, C. Block Copolymer Micelles as Switchable Templates for Nanofabrication. *Langmuir* **2006**, *22*, 3450−3452.
(52) Li, M. Q.; Ober, C. K. Block Copolymer Patterns and Templates. *Mater. Today* **2006**, *9*, 30−39.
(53) Hamley, I. W. Nanostructure Fabrication Using Block Copolymers. *Nanotechnology* **2003**, *14*, R39−R54.
(54) Bockstaller, M. R.; Mickiewicz, R. A.; Thomas, E. L. Block Copolymer Nanocomposites: Perspectives for Tailored Functional Materials. *Adv. Mater.* **2005**, *17*, 1331−1349.
(55) Bang, J.; Jeong, U.; Ryu, D. Y.; Russell, T. P.; Hawker, C. J. Block Copolymer Nanolithography: Translation of Molecular Level Control to Nanoscale Patterns. *Adv. Mater.* **2009**, *21*, 4769−4792.
(56) Choi, J. W.; Kim, M.; Safron, N. S.; Arnold, M. S.; Gopalan, P. Transfer of Pre-Assembled Block Copolymer Thin Film to Nano-pattern Unconventional Substrates. *ACS Appl. Mater. Interfaces* **2014**, *6*, 9442−9448.
(57) George, A.; Maijenburg, A. W.; Maas, M. G.; Blank, D. H. A.; ten Elshof, J. E. Electrodeposition in Capillaries: Bottom-up Micro- and Nanopatterning of Functional Materials on Conductive Substrates. *ACS Appl. Mater. Interfaces* **2011**, *3*, 3666−3672.
(58) Sjöström, T.; McNamara, L. E.; Yang, L.; Dalby, M. J.; Su, B. Novel Anodization Technique Using a Block Copolymer Template for Nanopatterning of Titanium Implant Surfaces. *ACS Appl. Mater. Interfaces* **2012**, *4*, 6354−6361.
(59) Suresh, V.; Huang, M. S.; Srinivasan, M. P.; Krishnamoorthy, S. In Situ Synthesis of High Density Sub-50 Nm Zno Nanopatterned Arrays Using Diblock Copolymer Templates. *ACS Appl. Mater. Interfaces* **2013**, *5*, 5727−5732.
(60) Park, M.; Harrison, C.; Chaikin, P. M.; Register, R. A.; Adamson, D. H. Block Copolymer Lithography: Periodic Arrays of Similar to 10(11) Holes in 1 Square Centimeter. *Science* **1997**, *276*, 1401−1404.
(61) Ludwigs, S.; Boker, A.; Voronov, A.; Rehse, N.; Magerle, R.; Krausch, G. Self-Assembly of Functional Nanostructures from ABC triblock copolymers. *Nat. Mater.* **2003**, *2*, 744−747.
(62) Kim, J. K.; Lee, J. I.; Lee, D. H. Self-Assembled Block Copolymers: Bulk to Thin Film. *Macromol. Res.* **2008**, *16*, 267−292.
(63) Park, C.; Yoon, J.; Thomas, E. L. Enabling Nanotechnology with Self Assembled Block Copolymer Patterns. *Polymer* **2003**, *44*, 6725−6760.
(64) Schultz, A. J.; Hall, C. K.; Genzer, J. Computer Simulation of Block Copolymer/Nanoparticle Composites. *Macromolecules* **2005**, *38*, 3007−3016.
(65) Xu, T.; Stevens, J.; Villa, J. A.; Goldbach, J. T.; Guarim, K. W.; Black, C. T.; Hawker, C. J.; Russell, T. R. Block Copolymer Surface Reconstuction: A Reversible Route to Nanoporous Films. *Adv. Funct. Mater.* **2003**, *13*, 698−702.
(66) Thurn-Albrecht, T.; Schotter, J.; Kastle, C. A.; Emley, N.; Shibauchi, T.; Krusin-Elbaum, L.; Guarini, K.; Black, C. T.; Tuominen, M. T.; Russell, T. P. Ultrahigh-Density Nanowire Arrays Grown in Self-Assembled Diblock Copolymer Templates. *Science* **2000**, *290*, 2126−2129.
(67) Xu, T.; Goldbach, J. T.; Misner, M. J.; Kim, S.; Gibaud, A.; Gang, O.; Ocko, B.; Guarini, K. W.; Black, C. T.; Hawker, C. J.; Russell, T. P. Scattering Study on the Selective Solvent Swelling Induced Surface Reconstruction. *Macromolecules* **2004**, *37*, 2972−2977.
(68) Black, C. T. Polymer Self-Assembly as a Novel Extension to Optical Lithography. *ACS Nano* **2007**, *1*, 147−150.
(69) Gowd, E. B.; Nandan, B.; Vyas, M. K.; Bigall, N. C.; Eychmüller, A.; Schloerb, H.; Stamm, M. Highly Ordered Palladium Nanodots and Nanowires from Switchable Block Copolymer Thin Films. *Nanotechnology* **2009**, *20*, 415302 (415310pp)..

DOI: 10.1021/am507567q
ACS Appl. Mater. Interfaces 2015, 7, 12559−12569

(70) Darling, S. B. Directing the Self-Assembly of Block Copolymers. *Prog. Polym. Sci.* **2007**, *32*, 1152−1204.
(71) Ruzette, A. V.; Leibler, L. Block Copolymers in Tomorrow's Plastics. *Nat. Mater.* **2005**, *4*, 19−31.
(72) Bates, F. S.; Fredrickson, G. H. Block Copolymers - Designer Soft Materials. *Phys. Today* **1999**, *52*, 32−38.
(73) Krausch, G.; Magerle, R. Nanostructured Thin Films Via Self-Assembly of Block Copolymers. *Adv. Mater.* **2002**, *14*, 1579−1583.
(74) Han, E.; Stuen, K. O.; Leolukman, M.; Liu, C.-C.; Nealey, P. F.; Gopalan, P. Perpendicular Orientation of Domains in Cylinder-Forming Block Copolymer Thick Films by Controlled Interfacial Interactions. *Macromolecules* **2009**, *42*, 4896−4901.
(75) Sinturel, C.; Vayer, M.; Morris, M.; Hillmyer, M. A. Solvent Vapor Annealing of Block Polymer Thin Films. *Macromolecules* **2013**, *46*, 5399−5415.
(76) Gowd, E. B.; Koga, T.; Endoh, M. K.; Kumar, K.; Stamm, M. Pathways of Cylindrical Orientations in Ps-B-P4vp Diblock Copolymer Thin Films Upon Solvent Vapor Annealing. *Soft Matter* **2014**, *10*, 7753−7761.
(77) Tokarev, I.; Krenek, R.; Burkov, Y.; Schmeisser, D.; Sidorenko, A.; Minko, S.; Stamm, M. Microphase Separation in Thin Films of Poly(Styrene-Block-4-Vinylpyridine) Copolymer−2-(4′-Hydroxybenzeneazo)Benzoic Acid Assembly. *Macromolecules* **2004**, *38*, 507−516.
(78) Thurn-Albrecht, T.; Steiner, R.; DeRouchey, J.; Stafford, C. M.; Huang, E.; Bal, M.; Tuominen, M.; Hawker, C. J.; Russell, T. Nanoscopic Templates from Oriented Block Copolymer Films. *Adv. Mater.* **2000**, *12*, 787−791.
(79) Sidorenko, A.; Tokarev, I.; Minko, S.; Stamm, M. Ordered Reactive Nanomembranes/Nanotemplates from Thin Films of Block Copolymer Supramolecular Assembly. *J. Am. Chem. Soc.* **2003**, *125*, 12211−12216.
(80) Nandan, B.; Gowd, E. B.; Bigall, N. C.; Eychmüller, A.; Formanek, P.; Simon, P.; Stamm, M. Arrays of Inorganic Nanodots and Nanowires Using Nanotemplates Based on Switchable Block Copolymer Supramolecular Assemblies. *Adv. Funct. Mater.* **2009**, *19*, 2805−2811.
(81) Luchnikov, V.; Kondyurin, A.; Formanek, P.; Lichte, H.; Stamm, M. Moire Patterns in Superimposed Nanoporous Thin Films Derived from Block-Copolymer Assemblies. *Nano Lett.* **2007**, *7*, 3628−3632.
(82) Park, S.; Wang, J. Y.; Kim, B.; Russell, T. P. From Nanorings to Nanodots by Patterning with Block Copolymers. *Nano Lett.* **2008**, *8*, 1667−1672.
(83) Shin, K.; Leach, K. A.; Goldbach, J. T.; Kim, D. H.; Jho, J. Y.; Tuominen, M.; Hawker, C. J.; Russell, T. P. A Simple Route to Metal Nanodots and Nanoporous Metal Films. *Nano Lett.* **2002**, *2*, 933−936.
(84) Seifarth, O.; Krenek, R.; Tokarev, I.; Burkov, Y.; Sidorenko, A.; Minko, S.; Stamm, M.; Schmeisser, D. Metallic Nickel Nanorod Arrays Embedded into Ordered Block Copolymer Templates. *Thin Solid Films* **2007**, *515*, 6552−6556.
(85) Crossland, E. J. W.; Ludwigs, S.; Hillmyer, M. A.; Steiner, U. Freestanding Nanowire Arrays from Soft-Etch Block Copolymer Templates. *Soft Matter* **2007**, *3*, 94−98.
(86) Ras, R. H. A.; Kemell, M.; de Wit, J.; Ritala, M.; ten Brinke, G.; Leskela, M.; Ikkala, O. Hollow Inorganic Nanospheres and Nanotubes with Tunable Wall Thicknesses by Atomic Layer Deposition on Self-Assembled Polymeric Templates. *Adv. Mater.* **2007**, *19*, 102−106.
(87) Mistark, P. A.; Park, S.; Yalcin, S. E.; Lee, D. H.; Yavuzcetin, O.; Tuominen, M. T.; Russell, T. P.; Achermann, M. Block-Copolymer-Based Plasmonic Nanostructures. *ACS Nano* **2009**, *3*, 3987−3992.
(88) Smarsly, B.; Grosso, D.; Brezesinski, T.; Pinna, N.; Boissiere, C.; Antonietti, M.; Sanchez, C. Highly Crystalline Cubic Mesoporous TiO_2 with 10-nm Pore Diameter Made with a New Block Copolymer Template. *Chem. Mater.* **2004**, *16*, 2948−2952.
(89) Forster, S.; Plantenberg, T. From Self-Organizing Polymers to Nanohybrid and Biomaterials. *Angew. Chem., Int. Ed.* **2002**, *41*, 689−714.
(90) Chai, J.; Buriak, J. M. Using Cylindrical Domains of Block Copolymers to Self-Assemble and Align Metallic Nanowires. *ACS Nano* **2008**, *2*, 489−501.
(91) Chai, J.; Wang, D.; Fan, X. N.; Buriak, J. M. Assembly of Aligned Linear Metallic Patterns on Silicon. *Nat. Nanotechnol.* **2007**, *2*, 500−506.
(92) Ethirajan, A.; Wiedwald, U.; Boyen, H. G.; Kern, B.; Han, L.; Klimmer, A.; Weigl, F.; Kästle, G.; Ziemann, P.; Fauth, K.; Cai, J.; Behm, R. J.; Romanyuk, A.; Oelhafen, P.; Walther, P.; Biskupek, J.; Kaiser, U. A Micellar Approach to Magnetic Ultrahigh-Density Data-Storage Media: Extending the Limits of Current Colloidal Methods. *Adv. Mater.* **2007**, *19*, 406−410.
(93) Härtling, T.; Uhlig, T.; Seidenstuecker, A.; Bigall, N. C.; Olk, P.; Wiedwald, U.; Han, L.; Eychmüller, A.; Plettl, A.; Ziemann, P.; Eng, L. M. Fabrication of Two-Dimensional Au@Fept Core-Shell Nanoparticle Arrays by Photochemical Metal Deposition. *Appl. Phys. Lett.* **2010**, *96*, 183111 (183113pp)..
(94) Park, S.; Kim, B.; Wang, J. Y.; Russell, T. P. Fabrication of Highly Ordered Silicon Oxide Dots and Stripes from Block Copolymer Thin Films. *Adv. Mater.* **2008**, *20*, 681−685.
(95) Lo, K. H.; Tseng, W. H.; Ho, R. M. In-Situ Formation of Cds Nanoarrays by Pore-Filling Nanoporous Templates from Degradable Block Copolymers. *Macromolecules* **2007**, *40*, 2621−2624.
(96) Spatz, J. P.; Herzog, T.; Mossmer, S.; Ziemann, P.; Möller, M. Micellar Inorganic-Polymer Hybrid Systems - a Tool for Nanolithography. *Adv. Mater.* **1999**, *11*, 149−153.
(97) Boyen, H. G.; Kastle, G.; Zurn, K.; Herzog, T.; Weigl, F.; Ziemann, P.; Mayer, O.; Jerome, C.; Möller, M.; Spatz, J. P.; Garnier, M. G.; Oelhafen, P. A Micellar Route to Ordered Arrays of Magnetic Nanoparticles: From Size-Selected Pure Cobalt Dots to Cobalt-Cobalt Oxide Core-Shell Systems. *Adv. Funct. Mater.* **2003**, *13*, 359−364.
(98) Ansari, I. A.; Hamley, I. W. Templating the Patterning of Gold Nanoparticles Using a Stained Triblock Copolymer Film Surface. *J. Mater. Chem.* **2003**, *13*, 2412−2413.
(99) Kastle, G.; Boyen, H. G.; Weigl, F.; Lengl, G.; Herzog, T.; Ziemann, P.; Riethmuller, S.; Mayer, O.; Hartmann, C.; Spatz, J. P.; Möller, M.; Ozawa, M.; Banhart, F.; Garnier, M. G.; Oelhafen, P. Micellar Nanoreactors - Preparation and Characterization of Hexagonally Ordered Arrays of Metallic Nanodots. *Adv. Funct. Mater.* **2003**, *13*, 853−861.
(100) Kim, D. H.; Kim, S. H.; Lavery, K.; Russell, T. P. Inorganic Nanodots from Thin Films of Block Copolymers. *Nano Lett.* **2004**, *4*, 1841−1844.
(101) Boontongkong, Y.; Cohen, R. E. Cavitated Block Copolymer Micellar Thin Films: Lateral Arrays of Open Nanoreactors. *Macromolecules* **2002**, *35*, 3647−3652.
(102) Spatz, J. P.; Roescher, A.; Möller, M. Gold Nanoparticles in Micellar Poly(Styrene)-B-Poly(Ethylene Oxide) Films-Size and Interparticle Distance Control in Monoparticulate Films. *Adv. Mater.* **1996**, *8*, 337−340.
(103) Spatz, J. P.; Roescher, A.; Sheiko, S.; Krausch, G.; Möller, M. Noble-Metal Loaded Block Ionomers - Micelle Organization, Adsorption of Free Chains and Formation of Thin-Films. *Adv. Mater.* **1995**, *7*, 731−735.
(104) Lohmueller, T.; Bock, E.; Spatz, J. P. Synthesis of Quasi-Hexagonal Ordered Arrays of Metallic Nanoparticles with Tuneable Particle Size. *Adv. Mater.* **2008**, *20*, 2297−2302.
(105) Abes, J. I.; Cohen, R. E.; Ross, C. A. Selective Growth of Cobalt Nanoclusters in Domains of Block Copolymer Films. *Chem. Mater.* **2003**, *15*, 1125−1131.
(106) Yun, S. H.; Sohn, B. H.; Jung, J. C.; Zin, W. C.; Lee, J. K.; Song, O. Tunable Magnetic Arrangement of Iron Oxide Nanoparticles in Situ Synthesized on the Solid Substrate from Diblock Copolymer Micelles. *Langmuir* **2005**, *21*, 6548−6552.
(107) Horiuchi, S.; Fujita, T.; Hayakawa, T.; Nakao, Y. Three-Dimensional Nanoscale Alignment of Metal Nanoparticles Using Block Copolymer Films as Nanoreactors. *Langmuir* **2003**, *19*, 2963−2973.

DOI: 10.1021/am507567q
ACS Appl. Mater. Interfaces 2015, 7, 12559−12569

(108) Lopes, W. A.; Jaeger, H. M. Hierarchical Self-Assembly of Metal Nanostructures on Diblock Copolymer Scaffolds. *Nature* **2001**, *414*, 735−738.
(109) Cheng, J. Y.; Ross, C. A.; Chan, V. Z. H.; Thomas, E. L.; Lammertink, R. G. H.; Vancso, G. J. Formation of a Cobalt Magnetic Dot Array Via Block Copolymer Lithography. *Adv. Mater.* **2001**, *13*, 1174−1178.
(110) Park, S.; Wang, J. Y.; Kim, B.; Xu, J.; Russell, T. P. A Simple Route to Highly Oriented and Ordered Nanoporous Block Copolymer Templates. *ACS Nano* **2008**, *2*, 766−772.
(111) Metwalli, E.; Couet, S.; Schlage, K.; Röhlsberger, R.; Körstgens, V.; Ruderer, M.; Wang, W.; Kaune, G.; Roth, S. V.; Müller-Buschbaum, P. In Situ Gisaxs Investigation of Gold Sputtering onto a Polymer Template. *Langmuir* **2008**, *24*, 4265−4272.
(112) Schlage, K.; Couet, S.; Roth, S. V.; Vainio, U.; Rüffer, R.; Kashem, M. M. A.; Müller-Buschbaum, P.; Röhlsberger, R. The Formation and Magnetism of Iron Nanostructures on Ordered Polymer Templates. *New J. Phys.* **2012**, *14*, 043007 (043013pp)..
(113) Metwalli, E.; Körstgens, V.; Schlage, K.; Meier, R.; Kaune, G.; Buffet, A.; Couet, S.; Roth, S. V.; Röhlsberger, R.; Müller-Buschbaum, P. Cobalt Nanoparticles Growth on a Block Copolymer Thin Film: A Time-Resolved Gisaxs Study. *Langmuir* **2013**, *29*, 6331−6340.
(114) Metwalli, E.; Moulin, J. F.; Perlich, J.; Wang, W.; Diethert, A.; Roth, S. V.; Müller-Buschbaum, P. Polymer-Template-Assisted Growth of Gold Nanowires Using a Novel Flow-Stream Technique. *Langmuir* **2009**, *25*, 11815−11821.
(115) Al-Hussein, M.; Schindler, M.; Ruderer, M. A.; Perlich, J.; Schwartzkopf, M.; Herzog, G.; Heidmann, B.; Buffet, A.; Roth, S. V.; Müller-Buschbaum, P. In Situ X-Ray Study of the Structural Evolution of Gold Nano-Domains by Spray Deposition on Thin Conductive P3ht Films. *Langmuir* **2013**, *29*, 2490−2497.
(116) Sarkar, K.; Braden, E. V.; Pogorzalek, S.; Yu, S.; Roth, S. V.; Müller-Buschbaum, P. Monitoring Structural Dynamics of in Situ Spray-Deposited Zinc Oxide Films for Application in Dye-Sensitized Solar Cells. *ChemSusChem* **2014**, *7*, 2140−2145.
(117) Otto, T.; Mundra, P.; Schelter, M.; Frolova, E.; Dorfs, D.; Gaponik, N.; Eychmüller, A. Application Prospects of Spray-Assisted Layer-by-Layer Assembly of Colloidal Nanoparticles. *ChemPhysChem* **2012**, *13*, 2128−2132.
(118) Misner, M. J.; Skaff, H.; Emrick, T.; Russell, T. P. Directed Deposition of Nanoparticles Using Diblock Copolymer Templates. *Adv. Mater.* **2003**, *15*, 221−224.
(119) Darling, S. B.; Yufa, N. A.; Cisse, A. L.; Bader, S. D.; Sibener, S. J., Self-Organization of Fept Nanoparticles on Photochemically Modified Diblock Copolymer Templates. *Adv. Mater.* **2005**, *17*, 2446-+.
(120) Horiuchi, S.; Sarwar, M. I.; Nakao, Y. Nanoscale Assembly of Metal Clusters in Block Copolymer Films with Vapor of a Metal-Acetylacetonato Complex Using a Dry Process. *Adv. Mater.* **2000**, *12*, 1507−1511.
(121) Watanabe, S.; Fujiwara, R.; Hada, M.; Okazaki, Y.; Iyoda, T. Site-Specific Recognition of Nanophase-Separated Surfaces of Amphiphilic Block Copolymers by Hydrophilic and Hydrophobic Gold Nanoparticles. *Angew. Chem., Int. Ed.* **2007**, *46*, 1120−1123.
(122) Tsutsumi, K.; Funaki, Y.; Hirokawa, Y.; Hashimoto, T. Selective Incorporation of Palladium Nanoparticles into Microphase-Separated Domains of Poly(2-Vinylpyridine)-Block-Polyisoprene. *Langmuir* **1999**, *15*, 5200−5203.
(123) Chiu, J. J.; Kim, B. J.; Kramer, E. J.; Pine, D. J. Control of Nanoparticle Location in Block Copolymers. *J. Am. Chem. Soc.* **2005**, *127*, 5036−5037.
(124) Minelli, C.; Hinderling, C.; Heinzelmann, H.; Pugin, R.; Liley, M. Micrometer-Long Gold Nanowires Fabricated Using Block Copolymer Templates. *Langmuir* **2005**, *21*, 7080−7082.
(125) Zhang, Q. L.; Xu, T.; Butterfield, D.; Misner, M. J.; Ryu, D. Y.; Emrick, T.; Russell, T. P. Controlled Placement of Cdse Nanoparticles in Diblock Copolymer Templates by Electrophoretic Deposition. *Nano Lett.* **2005**, *5*, 357−361.
(126) Peng, X. G.; Manna, L.; Yang, W. D.; Wickham, J.; Scher, E.; Kadavanich, A.; Alivisatos, A. P. Shape Control of Cdse Nanocrystals. *Nature* **2000**, *404*, 59−61.
(127) Manna, L.; Milliron, D. J.; Meisel, A.; Scher, E. C.; Alivisatos, A. P. Controlled Growth of Tetrapod-Branched Inorganic Nanocrystals. *Nat. Mater.* **2003**, *2*, 382−385.
(128) Carbone, L.; Cozzoli, P. D. Colloidal Heterostructured Nanocrystals: Synthesis and Growth Mechanisms. *Nano Today* **2010**, *5*, 449−493.
(129) Banin, U.; Ben-Shahar, Y.; Vinokurov, K. Hybrid Semiconductor-Metal Nanoparticles: From Architecture to Function. *Chem. Mater.* **2014**, *26*, 97−110.
(130) Lee, N.; Hyeon, T. Designed Synthesis of Uniformly Sized Iron Oxide Nanoparticles for Efficient Magnetic Resonance Imaging Contrast Agents. *Chem. Soc. Rev.* **2012**, *41*, 2575−2589.
(131) Sun, S. H.; Zeng, H.; Robinson, D. B.; Raoux, S.; Rice, P. M.; Wang, S. X.; Li, G. X. Monodisperse Mfe2o4 (M = Fe, Co, Mn) Nanoparticles. *J. Am. Chem. Soc.* **2004**, *126*, 273−279.
(132) Brown, K. R.; Walter, D. G.; Natan, M. J. Seeding of Colloidal Au Nanoparticle Solutions. 2. Improved Control of Particle Size and Shape. *Chem. Mater.* **2000**, *12*, 306−313.
(133) Grabar, K. C.; Brown, K. R.; Keating, C. D.; Stranick, S. J.; Tang, S. L.; Natan, M. J. Nanoscale Characterization of Gold Colloid Monolayers: A Comparison of Four Techniques. *Anal. Chem.* **1997**, *69*, 471−477.
(134) Bigall, N. C.; Reitzig, M.; Naumann, W.; Simon, P.; van Pee, K. H.; Eychmüller, A. Fungal Templates for Noble-Metal Nanoparticles and Their Application in Catalysis. *Angew. Chem., Int. Ed.* **2008**, *47*, 7876−7879.
(135) Gowd, E. B.; Nandan, B.; Bigall, N. C.; Eychmüller, A.; Formanek, P.; Stamm, M. Hexagonally Ordered Arrays of Metallic Nanodots from Thin Films of Functional Block Copolymers. *Polymer* **2010**, *51*, 2661−2667.
(136) Park, S. C.; Kim, B. J.; Hawker, C. J.; Kramer, E. J.; Bang, J.; Ha, J. S. Controlled Ordering of Block Copolymer Thin Films by the Addition of Hydrophilic Nanoparticles. *Macromolecules* **2007**, *40*, 8119−8124.
(137) Ploshnik, E.; Salant, A.; Banin, U.; Shenhar, R., Hierarchical Surface Patterns of Nanorods Obtained by Co-Assembly with Block Copolymers in Ultrathin Films. *Adv. Mater.* **2010**, *22*, 2774-+.
(138) Horechyy, A.; Zafeiropoulos, N. E.; Nandan, B.; Formanek, P.; Simon, F.; Kiriy, A.; Stamm, M. Highly Ordered Arrays of Magnetic Nanoparticles Prepared Via Block Copolymer Assembly. *J. Mater. Chem.* **2010**, *20*, 7734−7741.
(139) Kim, B. J.; Bang, J.; Hawker, C. J.; Kramer, E. J. Effect of Areal Chain Density on the Location of Polymer-Modified Gold Nanoparticles in a Block Copolymer Template. *Macromolecules* **2006**, *39*, 4108−4114.
(140) Zhao, Y.; Thorkelsson, K.; Mastroianni, A. J.; Schilling, T.; Luther, J. M.; Rancatore, B. J.; Matsunaga, K.; Jinnai, H.; Wu, Y.; Poulsen, D.; Frechet, J. M. J.; Alivisatos, A. P.; Xu, T. Small-Molecule-Directed Nanoparticle Assembly Towards Stimuli-Responsive Nanocomposites. *Nat. Mater.* **2009**, *8*, 979−985.
(141) Garcia, I.; Tercjak, A.; Zafeiropoulos, N. E.; Stamm, M.; Mondragon, I. Self-Assembling Nanomaterials Using Magnetic Nanoparticles Modified with Polystyrene Brushes. *Macromol. Rapid Commun.* **2007**, *28*, 2361−2365.
(142) Kashem, M. M. A.; Perlich, J.; Diethert, A.; Wang, W. N.; Memesa, M.; Gutmann, J. S.; Majkova, E.; Capek, I.; Roth, S. V.; Petry, W.; Muller-Buschbaum, P. Array of Magnetic Nanoparticles Via Particle Co-Operated Self-Assembly in Block Copolymer Thin Film. *Macromolecules* **2009**, *42*, 6202−6208.
(143) Li, Q. F.; He, J. B.; Glogowski, E.; Li, X. F.; Wang, J.; Emrick, T.; Russell, T. P. Responsive Assemblies: Gold Nanoparticles with Mixed Ligands in Microphase Separated Block Copolymers. *Adv. Mater.* **2008**, *20*, 1462−1466.
(144) Balazs, A. C.; Emrick, T.; Russell, T. P. Nanoparticle Polymer Composites: Where Two Small Worlds Meet. *Science* **2006**, *314*, 1107−1110.

DOI: 10.1021/am507567q
ACS Appl. Mater. Interfaces 2015, 7, 12559−12569

(145) Chen, H. Y.; Ruckenstein, E. Nanoparticle Aggregation in the Presence of a Block Copolymer. *J. Chem. Phys.* **2009**, *131*, 244904 (244907pp)..
(146) Chen, H. Y.; Ruckenstein, E. Structure and Particle Aggregation in Block Copolymer-Binary Nanoparticle Composites. *Polymer* **2010**, *51*, 5869−5882.
(147) Koh, H. D.; Park, S.; Russell, T. P. Fabrication of Pt/Au Concentric Spheres from Triblock Copolymer. *ACS Nano* **2010**, *4*, 1124−1130.
(148) Acharya, H.; Sung, J.; Sohn, B. H.; Kim, D. H.; Tamada, K.; Park, C. Tunable Surface Plasmon Band of Position Selective Ag and Au Nanoparticles in Thin Block Copolymer Micelle Films. *Chem. Mater.* **2009**, *21*, 4248−4255.
(149) Huang, C. M.; Wei, K. H. Pseudo-Single-Crystalline Self-Assembled Structure Formed from Hydrophilic Cdse and Hydrophobic an Nanoparticles in the Polystyrene and Poly(4-Vinylpyridine) Blocks, Respectively, of a Polystyrene-B-Poly(4-Vinylpyridine) Diblock Copolymer. *Macromolecules* **2008**, *41*, 6876−6879.
(150) Horechyy, A.; Nandan, B.; Zafeiropoulos, N. E.; Formanek, P.; Oertel, U.; Bigall, N. C.; Eychmüller, A.; Stamm, M. A Step-Wise Approach for Dual Nanoparticle Patterning Via Block Copolymer Self-Assembly. *Adv. Funct. Mater.* **2013**, *23*, 483−490.
(151) Bockstaller, M. R.; Lapetnikov, Y.; Margel, S.; Thomas, E. L. Size-Selective Organization of Enthalpic Compatibilized Nanocrystals in Ternary Block Copolymer/Particle Mixtures. *J. Am. Chem. Soc.* **2003**, *125*, 5276−5277.
(152) Son, J. G.; Bae, W. K.; Kang, H. M.; Nealey, P. F.; Char, K. Placement Control of Nanomaterial Arrays on the Surface-Reconstructed Block Copolymer Thin Films. *ACS Nano* **2009**, *3*, 3927−3934.
(153) Sohn, B. H.; Choi, J. M.; Yoo, S. I.; Yun, S. H.; Zin, W. C.; Jung, J. C.; Kanehara, M.; Hirata, T.; Teranishi, T. Directed Self-Assembly of Two Kinds of Nanoparticles Utilizing Monolayer Films of Diblock Copolymer Micelles. *J. Am. Chem. Soc.* **2003**, *125*, 6368−6369.
(154) Shin, D. O.; Mun, J. H.; Hwang, G.-T.; Yoon, J. M.; Kim, J. Y.; Yun, J. M.; Yang, Y.-B.; Oh, Y.; Lee, J. Y.; Shin, J.; Lee, K. J.; Park, S.; Kim, J. U.; Kim, S. O. Multicomponent Nanopatterns by Directed Block Copolymer Self-Assembly. *ACS Nano* **2013**, *7*, 8899−8907.
(155) Hiramatsu, H.; Osterloh, F. E. A Simple Large-Scale Synthesis of Nearly Monodisperse Gold and Silver Nanoparticles with Adjustable Sizes and with Exchangeable Surfactants. *Chem. Mater.* **2004**, *16*, 2509−2511.
(156) Lin, Y.; Boker, A.; He, J. B.; Sill, K.; Xiang, H. Q.; Abetz, C.; Li, X. F.; Wang, J.; Emrick, T.; Long, S.; Wang, Q.; Balazs, A.; Russell, T. P. Self-Directed Self-Assembly of Nanoparticle/Copolymer Mixtures. *Nature* **2005**, *434*, 55−59.
(157) Thompson, R. B.; Ginzburg, V. V.; Matsen, M. W.; Balazs, A. C. Block Copolymer-Directed Assembly of Nanoparticles: Forming Mesoscopically Ordered Hybrid Materials. *Macromolecules* **2002**, *35*, 1060−1071.
(158) Thompson, R. B.; Ginzburg, V. V.; Matsen, M. W.; Balazs, A. C. Predicting the Mesophases of Copolymer-Nanoparticle Composites. *Science* **2001**, *292*, 2469−2472.
(159) Liz-Marzan, L. M. Tailoring Surface Plasmons through the Morphology and Assembly of Metal Nanoparticles. *Langmuir* **2006**, *22*, 32−41.
(160) Kim, B. J.; Chiu, J. J.; Yi, G. R.; Pine, D. J.; Kramer, E. J. Nanoparticle-Induced Phase Transitions in Diblock-Copolymer Films. *Adv. Mater.* **2005**, *17*, 2618−2622.
(161) Yeh, S. W.; Wei, K. H.; Sun, Y. S.; Jeng, U. S.; Liang, K. S. Cds Nanoparticles Induce a Morphological Transformation of Poly-(Styrene-B-4-Vinylpyridine) from Hexagonally Packed Cylinders to a Lamellar Structure. *Macromolecules* **2005**, *38*, 6559−6565.

DOI: 10.1021/am507567q
ACS Appl. Mater. Interfaces 2015, 7, 12559−12569